Received: 17 July 2021 | Revised: 1 November 2021 | Accepted: 3 November 2021

DOI: 10.1111/cas.15197

ORIGINAL ARTICLE

Cancer Science WILEY

Nuclear accumulation of KPNA2 impacts radioresistance through positive regulation of the PLSCR1-STAT1 loop in lung adenocarcinoma

Wei-Chao Liao[1,2] | Tsung-Jen Lin[3] | Yu-Chin Liu[1,3] | Yu-Shan Wei[4] | Guan-Ying Chen[3] | Hsiang-Pu Feng[4] | Yi-Feng Chang[1,5] | Hsin-Tzu Chang[1,3] | Chih-Liang Wang[6,7] | Hsinag-Cheng Chi[8,9] | Chun-I Wang[10] | Kwang-Huei Lin[4,11,12,13] | Wei-Ting Ou Yang[1] | Chia-Jung Yu[1,3,4,7]

[1]Molecular Medicine Research Center, Chang Gung University, Taoyuan, Taiwan

[2]Department of Nephrology, Chang Gung Memorial Hospital, Linkou Medical Center, Taoyuan, Taiwan

[3]Department of Cell and Molecular Biology, College of Medicine, Chang Gung University, Taoyuan, Taiwan

[4]Graduate Institute of Biomedical Sciences, College of Medicine, Chang Gung University, Taoyuan, Taiwan

[5]Department of Neurosurgery, Chang Gung Memorial Hospital, Taoyuan, Taiwan

[6]School of Medicine, College of Medicine, Chang Gung University, Taoyuan, Taiwan

[7]Department of Thoracic Medicine, Chang Gung Memorial Hospital, Taoyuan, Taiwan

[8]Graduate Institute of Integrated Medicine, China Medical University, Taichung, Taiwan

[9]Chinese Medicine Research Center, China Medical University, Taichung, Taiwan

[10]Radiation Biology Research Center, Institute for Radiological Research, Chang Gung University/Chang Gung Memorial Hospital, Taoyuan, Taiwan

[11]Department of Biochemistry, College of Medicine, Chang Gung University, Taoyuan, Taiwan

[12]Liver Research Center, Chang Gung Memorial Hospital, Taoyuan, Taiwan

[13]Research Center for Chinese Herbal Medicine, College of Human Ecology, Chang Gung University of Science and Technology, Taoyuan, Taiwan

Correspondence
Chia-Jung Yu, Department of Cell and Molecular Biology, College of Medicine, Chang Gung University, 259 Wen-Hwa 1st Road, Guishan District, Taoyuan, Taiwan.
Email: yucj1124@mail.cgu.edu.tw

Funding information
Featured Areas Research Center Program within the framework of the Higher Education Sprout Project by the Ministry of Education, Taiwan, Grant/Award Number: EMRPD1L0351; Chang Gung Memorial Hospital, Linkou, Grant/Award Number: BMRP894, CLRPD1J0013 and CMRPD1H0641-3

Abstract

Lung adenocarcinoma (ADC) is the predominant histological type of lung cancer, and radiotherapy is one of the current therapeutic strategies for lung cancer treatment. Unfortunately, biological complexity and cancer heterogeneity contribute to radioresistance development. Karyopherin α2 (KPNA2) is a member of the importin α family that mediates the nucleocytoplasmic transport of cargo proteins. KPNA2 overexpression is observed across cancer tissues of diverse origins. However, the role of KPNA2 in lung cancer radioresistance is unclear. Herein, we demonstrated that high expression of KPNA2 is positively correlated with radioresistance and cancer stem cell (CSC) properties in lung ADC cells. Radioresistant cells exhibited nuclear accumulation of KPNA2 and its cargos (OCT4 and c-MYC). Additionally, KPNA2 knockdown regulated CSC-related gene expression in radioresistant cells. Next-generation sequencing and bioinformatic analysis revealed that STAT1 activation and nuclear

Liao, Lin and Liu are contributed equally to this study.

This is an open access article under the terms of the Creative Commons Attribution-NonCommercial License, which permits use, distribution and reproduction in any medium, provided the original work is properly cited and is not used for commercial purposes.
© 2021 The Authors. *Cancer Science* published by John Wiley & Sons Australia, Ltd on behalf of Japanese Cancer Association.

phospholipid scramblase 1 (PLSCR1) are involved in KPNA2-mediated radioresistance. Endogenous PLSCR1 interacting with KPNA2 and PLSCR1 knockdown suppressed the radioresistance induced by KPNA2 expression. Both STAT1 and PLSCR1 were found to be positively correlated with dysregulated KPNA2 in radioresistant cells and ADC tissues. We further demonstrated a potential positive feedback loop between PLSCR1 and STAT1 in radioresistant cells, and this PLSCR1-STAT1 loop modulates CSC characteristics. In addition, AKT1 knockdown attenuated the nuclear accumulation of KPNA2 in radioresistant lung cancer cells. Our results collectively support a mechanistic understanding of a novel role for KPNA2 in promoting radioresistance in lung ADC cells.

KEYWORDS

cancer stem cell, KPNA2, lung cancer, PLSCR1, radioresistance

1 | INTRODUCTION

Lung cancer is one of the leading causes of cancer-related death worldwide, and adenocarcinoma (ADC) is the major histological type of lung cancer. Approximately 70% of patients are first diagnosed with lung cancer at an advanced stage,[1,2] which results in a poor survival rate within 5 years.[3] The conventional treatments for lung cancer include surgical resection, chemotherapy, targeted therapy and immunotherapy. Epidermal growth factor receptor (EGFR)-tyrosine kinase inhibitors (TKIs) have been used as targeted therapies in advanced ADC patients harboring EGFR mutations.[4] Unfortunately, all drugs inevitably face the problem of resistance.

Radiotherapy is one of the major therapeutic approaches in cancer, and more than 50% of patients are treated using this method.[5] In the past decade, with advancements in modern radiotherapy and functional imaging, the application of radiotherapy in the management of early-stage and advanced-stage non–small cell lung cancer (NSCLC), including ADC, has been greatly expanded. The therapeutic effects of radiotherapy arise from its ability to induce DNA damage in tumor tissues through reactive oxygen species (ROS) or direct ionization of DNA molecules. However, biological complexity and cancer heterogeneity contribute to the development of radioresistance in tumors. Notably, ionizing radiation has been shown to induce a cancer stem cell (CSC) phenotype, cellular metastasis, epithelial-mesenchymal transition (EMT), and oncogenic metabolism in cancer cells, which, in turn, contribute to radioresistance.[7,8]

Karyopherin α2 (KPNA2, also known as importin α1) is a member of the karyopherin α family and mediates the transport of signal-containing cargo proteins from the cytoplasm to the nucleus.[9,10] KPNA2 overexpression has been found in several types of cancers, such as breast, ovarian, cervical, colon and lung cancers.[11,12] Elevated levels of KPNA2 further cause cancer invasion and a poor prognosis in cancer patients.[11,13] Previously, we identified KPNA2 as a potential biomarker in lung ADC and observed that KPNA2 overexpression was associated with poor differentiation, metastasis, and cell growth.[14] Our study also showed that KPNA2 interacts with c-MYC, NBS1, pErk, vimentin, p53, and E2F1 in lung cancer,[15,16] which are highly correlated with radiotherapy response and CSC properties.[17,18] Recently, KPNA2 was reported to respond to radiation exposure in colorectal cancer cells.[19,20] However, the impacts of dysregulated KPNA2 on radioresistance and CSCs are still not clear, and there is little information related to lung cancer therapy. Therefore, we aimed to investigate the role and underlying mechanisms of KPNA2-mediated radioresistance in lung cancer.

2 | MATERIALS AND METHODS

2.1 | Antibodies

The commercially available primary antibodies used in this study included the following: anti–KPNA2 (sc-55538), anti–vimentin (sc-6260), anti–AKT 1 (sc-5298), anti–c-MYC (sc-70469), and anti–GAPDH (sc-32233), which were purchased from Santa Cruz; anti–ABCG2 (ab207732); anti–E-cadherin (ab40772), anti–OCT4 (ab19857), and anti–c-MYC (ab32072), which were purchased from Abcam; anti–phospho-AKT (Ser473; 4060), anti–STAT1 (9176), and anti–phospho-STAT3 (9145), which were purchased from Cell Signaling Technology; anti–PLSCR1 (11582-1-AP), anti–histone 3 (17169-1-AP), and anti–KPNA2 (10819-1-AP), which were purchased from Proteintech; and anti–β-actin (MAB1501) and anti–Myc (05-724), which were obtained from Millipore. The secondary antibodies used for western blotting included HRP-conjugated goat anti–rabbit and HRP-conjugated goat anti–mouse IgG antibodies purchased from Cytiva. Immunofluorescence staining was performed using Alexa Fluor 594- and Alexa Fluor 488-conjugated secondary antibodies purchased from Molecular Probes.

2.2 | Cell lines and cell culture

The human lung ADC cell line CL1-0, which harbors wild-type EGFR, was established from a poorly differentiated lung ADC patient[21] and generously provided by Professor Pan-Chyr Yang (Department of Internal Medicine, National Taiwan University Hospital, Taipei, Taiwan). PE089, a lung ADC cell line with EGFR exon 19 deletion, was derived from a female lung ADC patient and kindly provided by Professor Ko-Jiunn Liu (National Institute of Cancer Research, National Health Research Institutes, Tainan, Taiwan).[22] CL1-0 and PE089 cells were cultured in RPMI 1640 medium (Invitrogen) and MEM (Invitrogen), respectively. Both culture media contained 10% FBS (Gibco) and 1% penicillin/streptomycin (Gibco), and the cells were incubated at 37°C in a humidified atmosphere comprising 95% air/5% CO_2.

2.3 | Establishment of radioresistant lung cancer cell lines

To establish radioresistant cancer cell lines, X-ray irradiation was applied as described previously.[23] Briefly, cells were exposed to 6 Gray (Gy) radiation using a Gated RapidArc gamma ray source. Cells with higher ATP-binding cassette transporter G2 (ABCG2) activity were isolated via cell sorting using flow cytometry (BD FACSAria III Cell Sorter, BD Biosciences, USA). The detailed procedures for cell sorting are described in Appendix S1.

2.4 | Small interfering RNA transfection

Small interfering RNA (siRNAs) purchased from Dharmacon (Thermo Fisher Scientific) were used for gene knockdown as described previously.[15] At 24 hours after transfection, cells were harvested for western blotting or quantitative real-time PCR (qRT-PCR) analysis to confirm the gene knockdown efficiency. The siRNA sequences used in this study are listed in Table S1.

2.5 | Plasmid constructs and gene expression

To express KPNA2 in mammalian cells, the open reading frame of KPNA2 was obtained from CL1-0 cells by PCR, and a tdTomato-tagged KPNA2 plasmid (tdTomato-KPNA2) and a Myc-tagged KPNA2 (KPNA2-Myc) were constructed. The open reading frame of PLSCR1 was isolated from HEK293 cells by PCR amplification, and the fragment was cloned into a p3xFlag-Myc-CMV-26 expression vector (Merck KGaA, Darmstadt, Germany) for transient expression of PLSCR1 in mammalian cells (Flag-PLSCR1). Cells were transfected with plasmids using TurboFect reagents (Fermentas Thermo Fisher Scientific) according to the manufacturer's instructions. Stable clones expressing KPNA2 (TK4S) were established by selection with the antibiotic gentamycin (Sigma-Aldrich, St. Louis, MO, USA).

2.6 | Clonogenic cell survival assay

Cells were seeded in six-well plates. After culture for 24 h, the cells were irradiated (2, 4, 6, or 10 Gy) by using a Gated RapidArc gamma ray source. To assess colony formation, the irradiated cells were cultured for an additional 7-10 days. The colonies were fixed with a 10% acetic acid/methanol solution and then stained with a 0.5% crystal violet solution. Colonies containing more than 50 cells were recognized as one colony on images and analyzed under a Lionheart FX automated microscope (BioTek, Winooski).

2.7 | RNA extraction and quantitative RT-PCR

Total RNA was extracted from ADC cells, and cDNA was prepared for qRT-PCR analysis as described previously.[15] The sequences of the gene-specific primers used in this study are shown in Table S2.

2.8 | Immunofluorescence assay and image analysis

Immunofluorescence assay (IFA) was performed as described previously, and the details are provided in Appendix S1. The images obtained from the IFA were analyzed by using a Zeiss Axio Imager Z1 microscope (Carl Zeiss, Gottingen, Germany), and the nuclear-to-cytoplasmic (N/C) ratios representing the subcellular localization of target proteins were measured under a Lionheart FX automated microscope (BioTek).

2.9 | Western blotting

Western blotting was carried out as previously described.[24] The western blotting details are provided in Appendix S1.

2.10 | Immunoprecipitation assay

For immunoprecipitation (IP) of endogenous KPNA2 or PLSCR1 from CL1-0 and PE089 cell lines, cell lysates were extracted in NP-40 lysis buffer (1% NP-40, 20 mmol/L Tris-HCl (pH 7.5), 150 mmol/L NaCl, 1 mmol/L Na_3VO_4, 5 mmol/L EDTA (pH 8.0), 10% glycerol, protease inhibitor cocktail, and phosphatase inhibitor cocktail) and fractionated by centrifugation (10 000 *g*, 15 minutes at 4°C) to obtain cell lysates. Then, 2 mg protein of cell lysates was incubated with 2 μg of anti–KPNA2 antibody (sc-55538), anti–PLSCR1 antibody (11582-1-AP), control-mouse IgG (sc-2025), or control-rabbit IgG (12-370) together with 20 μL Dynabeads

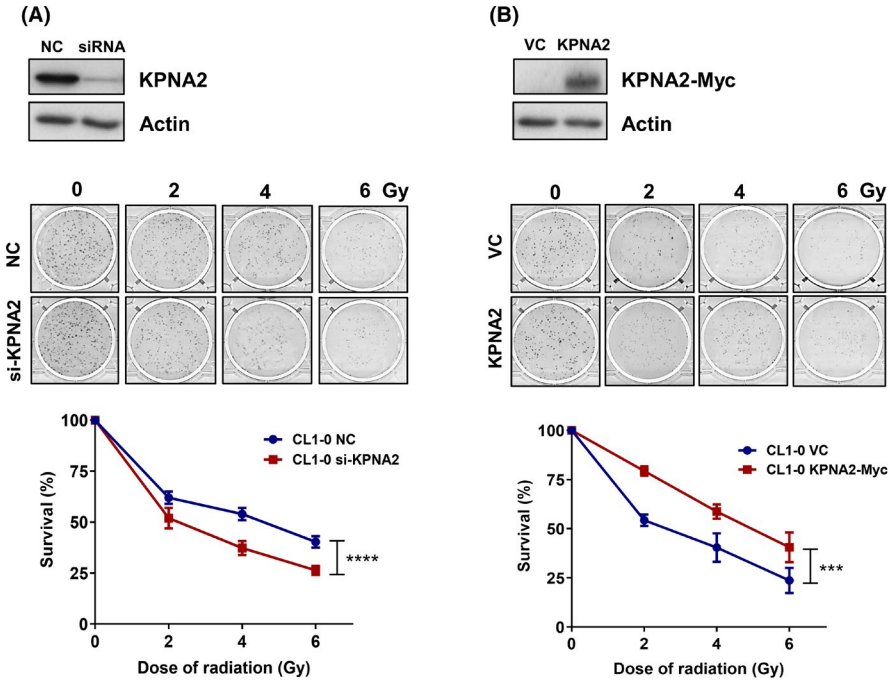

FIGURE 1 Karyopherin α2 (KPNA2) expression is correlated with radioresistance in lung adenocarcinoma (ADC) cells. Clonogenic survival assays performed with KPNA2-knockdown (A) and KPNA2-expressing (B) cells after exposure to different doses of radiation (0, 2, 4, and 6 Gy). Western blot analysis was used to determine KPNA2 expression levels in KPNA2-knockdown and KPNA2-expressing CL1-0 cells (upper panel). Actin was used as the internal control. NC, negative control siRNA. VC, vector control. The quantification of the clonogenic survival assays presented is shown in the lower panel. All of the data are presented as the mean ± SEM. ***$P < .001$ and ****$P < .0001$

protein G (Invitrogen). All incubations were performed with rotation overnight at 4°C, and the samples were then washed twice with Tris buffer A (20 mmol/L Tris-HCl (pH 7.5), 150 mmol/L NaCl (or 50 mmol/L NaCl), and 0.5 mmol/L DTT) and twice with Tris buffer B (20 mmol/L Tris-HCl (pH 7.5), and 0.5 mM DTT). The resulting protein complexes were eluted with SDS sample buffer and analyzed by western blotting.

2.11 | Subcellular fractionation

Cells were harvested with trypsin and washed thoroughly with PBS. The cell pellets were fractionated using the Nuclear Extraction Kit (Merck KGaA) according to the manufacturer's instructions. The fractionation efficacy was confirmed by western blotting using specific antibodies, including GAPDH (cytoplasmic marker) and histone 3 (nuclear marker).

2.12 | Next-generation sequencing and bioinformatic analysis

Next-generation sequencing (NGS) was performed as described in Appendix S1. Differentially expressed genes (DEG) with a two-fold change between control and treated cells were subjected to pathway analysis by using QIAGEN Ingenuity Pathway Analysis (IPA) software. The transcription factors (TF) involved in radioresistance and CSC regulation were predicted by using a manually curated database of human and mouse transcriptional regulatory networks, the Transcriptional Regulatory Relationships Unraveled by Sentence-based Text mining (TRRUST; version 2) system (https://www.grnpedia.org/trrust/).

2.13 | The Cancer Genome Atlas lung adenocarcinoma data analysis

Clinical information of lung ADC patients deposited in The Cancer Genome Atlas (TCGA-LUAD; ID: luad_tcga_pan_can_atlas_2018) was downloaded from the cBioPortal website (https://www.cbioportal.org/). The RNA-Seq raw read counts (HTSeq - Counts) of the Genomic Data Commons TCGA-LUAD were downloaded from the data repository of the UCSC Xena browser (https://gdc-hub.s3.us-east-1.amazonaws.com/download/TCGA-LUAD.htseq_counts.tsv.gz). We first performed inverse log2(RawCount + 1) transformation to convert the numeric expression values into integer raw count values. Next, we used DESeq2 (1.30.0) to convert the raw read counts into normalized counts. The ggscatter function of the ggpubr (0.4.0) R package was used to create scatter plots with the Spearman nonparametric statistic test.

2.14 | Statistical analysis

Prism 6.0 (GraphPad Software) statistical software packages were used for data analysis. All of the data are presented as the mean ± standard deviation (SD) or standard error of the mean (SEM). Two-way ANOVA and a two-tailed Student's *t* test were used for comparisons between control and experimental groups. Statistical significance was set at a *P*-value <.05 ($P < .05$).

3 | RESULTS

3.1 | KPNA2 expression is positively correlated with radioresistance in lung adenocarcinoma cells

To investigate the potential role of KPNA2 in the regulation of the lung ADC cell response to ionizing radiation, CL1-0 cells with knockdown or overexpression of KPNA2 were exposed to different doses of radiation (0, 2, 4 or 6 Gy) and then assessed in clonogenic cell survival assays. We determined the efficacy of siRNA-mediated KPNA2 knockdown or overexpression by western blotting (Figure 1A and B, upper panel). The colony formation numbers representing cell survival were decreased by radiation in a dose-dependent manner (0, 2, 4 and 6 Gy). Notably, the protein expression level of KPNA2 increased for 2 weeks upon irradiation exposure (6 Gy) (Figure S1A). Upon irradiation, the colony number was significantly decreased for KPNA2-knockdown cells compared with control cells (Figure 1A, lower panel). Consistently, colony numbers were increased for KPNA2-expressing cells compared to control cells after radiation exposure (Figure 1B, lower panel). These results collectively suggest that KPNA2 expression promotes radioresistance in lung ADC cells.

3.2 | Radioresistant cell lines exhibit dysregulated karyopherin α2 expression and cancer stem cell properties

To establish radioresistant cell lines, we isolated cells with high ABCG2 activity, a CSC characteristic, from irradiated cells by flow cytometry (Figure S1B) and used P2S2 (secondary sorting) when naming the cell lines. A clonogenic cell survival assay revealed that radioresistance was, indeed, increased in two sorted cell lines (CL1-0 P2S2 and PE089 P2S2) compared with the corresponding control cell lines (CL1-0 P0 and PE089 P0) (Figure 2A and B). We observed that the mRNA levels of ABCG2, KPNA2, E-cadherin, fibronectin, and OCT4 were significantly upregulated in these two sorted cell lines (Figure 2C). In addition, the mRNA level of vimentin was also upregulated in PE089 P2S2 cells. These results suggest that high expression of KPNA2 is positively correlated with CSC- and EMT-related gene expression in our established radioresistant lung ADC cell lines.

3.3 | Enhanced nuclear distributions of KPNA2, p-AKT, OCT4, and c-MYC in established radioresistant cells

Several lines of evidence show that KPNA2 is overexpressed and accumulates in the nucleus in human cancer cells.[11,12] Given the function of KPNA2 in the regulation of nucleocytoplasmic transport, a possible mechanism is that KPNA2 contributes to radioresistance through dysregulation of its cargo, such as the CSC markers OCT4 and c-MYC.[15,25] In addition, high activity of AKT/protein kinase B promotes radioresistance in NSCLC.[26-28] Therefore, we examined the subcellular distributions of KPNA2 and these radioresistance-related factors by using immunofluorescence and high-content image quantification. We observed that the p-AKT and KPNA2 signals

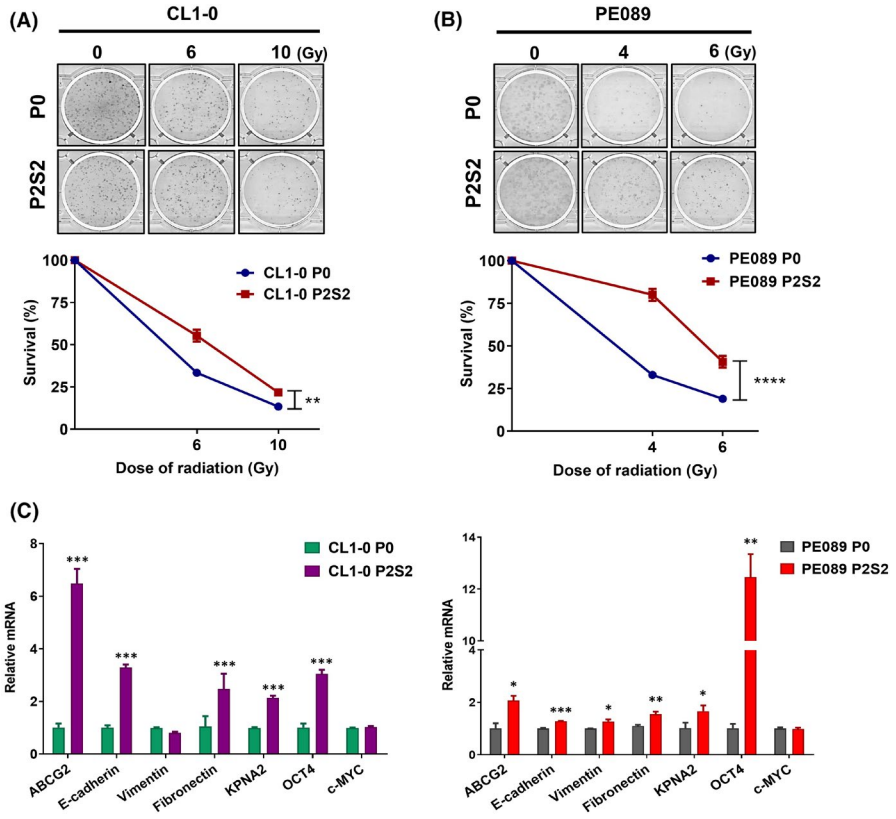

FIGURE 2 Establishment of radioresistant lung cancer cell lines with cancer stem cell (CSC) properties. Radioresistant P2S2 lung cancer cell lines, including CL1-0 (A) and PE089 (B) cell lines, were established by short-term fractionated irradiation followed by cell sorting as described in Appendix S1. Cells were exposed to different doses of radiation, followed by clonogenic survival assays (mean ± SEM). (C) EMT- and CSC-related gene expression in sorted cells was determined by quantitative RT-PCR. Data are presented as the mean ± SD of triplicate experiments. $^{*}P < .05$, $^{**}P < .01$, and $^{***}P < .001$

were enriched in the nuclear fractions of our two established P2S2 cell lines compared to those of control P0 cells (Figure 3A and C). The quantification of the nuclear and cytoplasmic distributions (N/C ratio) of interesting targets revealed that P2S2 cells had higher percentages of nuclear p-AKT and KPNA2 than control cells (Figure 3B and D). The enrichment of OCT4 and c-MYC in nuclear fractions was also observed in P2S2 cells, which supported the positive role of KPNA2 in regulating the nuclear entry of OCT4 and c-MYC in these radioresistant cells (Figure 3E-H). Although the signals of endogenous OCT4 and c-MYC were relatively low, the IP analysis demonstrated positive physical interactions between KPNA2 and these two endogenous transcription factors in lung ADC cells (Figure 3I). Consistently, the subcellular fractionation followed by western blotting further showed that the protein levels of KPNA2, OCT4, and c-MYC in the nuclear fractions were increased in these two P2S2 cell lines compared with the P0 cell lines (Figure 3J). Strong p-AKT signals were detected in the cytosolic fractions we tested via western blotting, and we still observed low but enriched signals of p-AKT in the nuclear fractions of these radioresistant cells. These results suggest that the nuclear accumulation of KPNA2 protein complexes and p-AKT may contribute to radioresistance in lung ADC cells.

3.4 | KPNA2 knockdown and KPNA2 expression induce alterations in radioresistance-related gene expression

Given that dysregulation of stemness-associated and EMT-related genes is often observed in radioresistant cells,[7,8,29] we examined the regulatory effect of KPNA2 on the expression of CSC- and EMT-related factors by quantitative PCR. As shown in Figure 4A, KPNA2 knockdown reduced the gene expression levels of CSC markers (ABCG2, OCT4, and c-MYC) in CL1-0 P2S2 cells. Similar results were observed in KPNA2-knockdown PE089 P2S2 cells (Figure 4A, lower panel). We then established CL1-0 lung cancer cell lines with stable KPNA2 expression (TK4S) and a control cell line (T1), and the mRNA levels of CSC- and EMT-associated genes were measured via qPCR to further confirm that KPNA2 promoted the gene expression of ABCG2, OCT4, and c-MYC but reduced the expression of E-cadherin (Figure 4B). These results support the idea that KPNA2 contributes to radioresistance by regulating CSC- and EMT-associated gene expression in lung cancer cells.

3.5 | Identification of the key regulators involved in KPNA2-mediated radioresistance via next-generation sequencing combined with bioinformatic analysis

To elucidate the mechanisms underlying KPNA2-mediated radioresistance, NGS was used to identify the DEGs in radioresistant KPNA2-knockdown cells and KPNA2-expressing cells. Figure 5A shows the intersection of the DEGs (>2-fold change) that were significantly upregulated in radioresistant cells and positively correlated with KPNA2 expression. This analysis revealed that 429 genes were potentially involved in KPNA2-mediated radioresistance. IPA showed that several upstream regulators, such as TNF-α, NF-κB, and STAT1, were involved in the regulation of the expression of the 429 genes (Table 1). The pathway network further demonstrated that extracellular functions, cytokines, and transcriptional regulators were major factors involved in promoting radioresistance (Figure 5B). Consistently, 14 TF, including the two well-known radioresistance- and/or CSC-related genes STAT1 and SP1,[30-35] were predicted to be the major TF involved in the transcriptional regulation of these 429 DEG according to the TRRUST database (Table S3). These results support the feasibility of NGS and bioinformatic analysis for identifying the key regulators involved in KPNA2-promoted radioresistance and CSC properties.

3.6 | STAT1 and PLSCR1 are positively correlated with dysregulated KPNA2 in radioresistant cells and adenocarcinoma tissues

Next-generation sequencing combined with bioinformatic analysis revealed that inflammatory cytokines and interferon (IFN) were the major upstream regulators involved in KPNA2-mediated radioresistance. Accumulating evidence supports the notion that targeting the IFN/STAT1 pathway would be a strategy to overcome radioresistance.[36] Notably, phospholipid scramblase PLSCR1, an IFN-inducible gene through STAT1 activation,[37] was reported as a KPNA2-interacting protein.[38] The PLSCR1-STAT3 heterodimer was recently reported to induce transcriptional activation of STAT1 in breast cancer cells.[39] We then hypothesized that KPNA2 regulates the nuclear entry of PLSCR1, which increases the STAT1 mRNA level and, thus, enhances the gene transcription of PLSCR1 in radioresistant lung ADC cells. Immunofluorescence staining showed that the

FIGURE 3 Enhanced nuclear distributions of karyopherin α2 (KPNA2), p-AKT, OCT4, and c-MYC were detected in radioresistant cells. The subcellular localization of KPNA2, p-AKT, OCT 4, and c-MYC in CL1-0 cells (A, E) and PE089 (C, G) cells was examined via immunofluorescence assay (IFA) using the indicated antibodies. Scale bars: 10 μm. (B, D, F, H) The distributions of target proteins in the nuclear (N) and cytoplasmic (C) fractions were analyzed under a Lionheart FX Automated Microscope ($n > 500$ for each group of cells). The N/C ratios of KPNA2, p-AKT, OCT 4, and c-MYC in CL1-0 (B, F) and PE089 (D, H) cells were analyzed. (I) The physical interaction between KPNA2 and its potential binding partners. Cell lysates from CL1-0 (left panel) and PE089 (right panel) cells were prepared for immunoprecipitation (IP) using anti–KPNA2 antibodies and control IgG, as described in the Materials and Methods. The resulting immunoprecipitated protein complexes were analyzed by western blotting using anti–KPNA2, anti–OCT4, anti–c-MYC, and anti–GAPDH antibodies as indicated. GAPDH was used as the internal control. (J) The protein levels of KPNA2, pAKT (Ser 473), OCT4, and c-MYC in the nuclear fractions were increased in P2S2 cell lines compared with the P0 cell lines. The cells were harvested and subjected to subcellular fractionation, followed by western blotting using the target-specific antibodies as indicated. GAPDH and histone 3 were used as loading controls for the cytosolic and nuclear fractions, respectively. Cy, cytosolic fraction; Nu, nuclear fraction; Wc, whole cell lysates

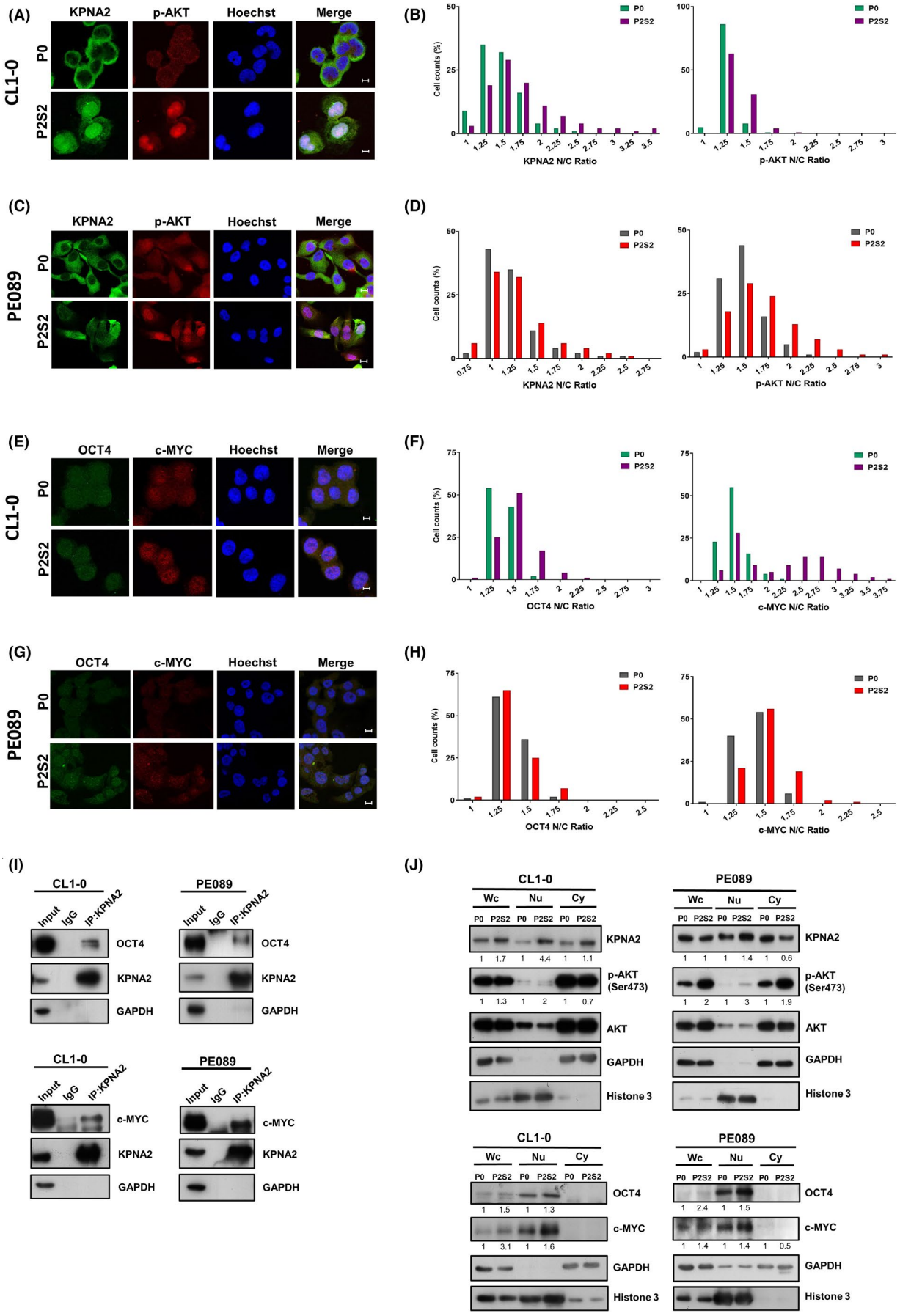
(A)
KPNA2
p-AKT
Hoechst
Merge
CL1-0
P0
P2S2
(B)
P0
P2S2
Cell counts (%)
KPNA2 N/C Ratio
p-AKT N/C Ratio
(C)
PE089
(D)
(E)
OCT4
c-MYC
OCT4 N/C Ratio
c-MYC N/C Ratio
(F)
(G)
(H)
(I)
CL1-0
PE089
Input
IgG
IP:KPNA2
OCT4
KPNA2
GAPDH
c-MYC
(J)
Wc
Nu
Cy
p-AKT (Ser473)
AKT
Histone 3

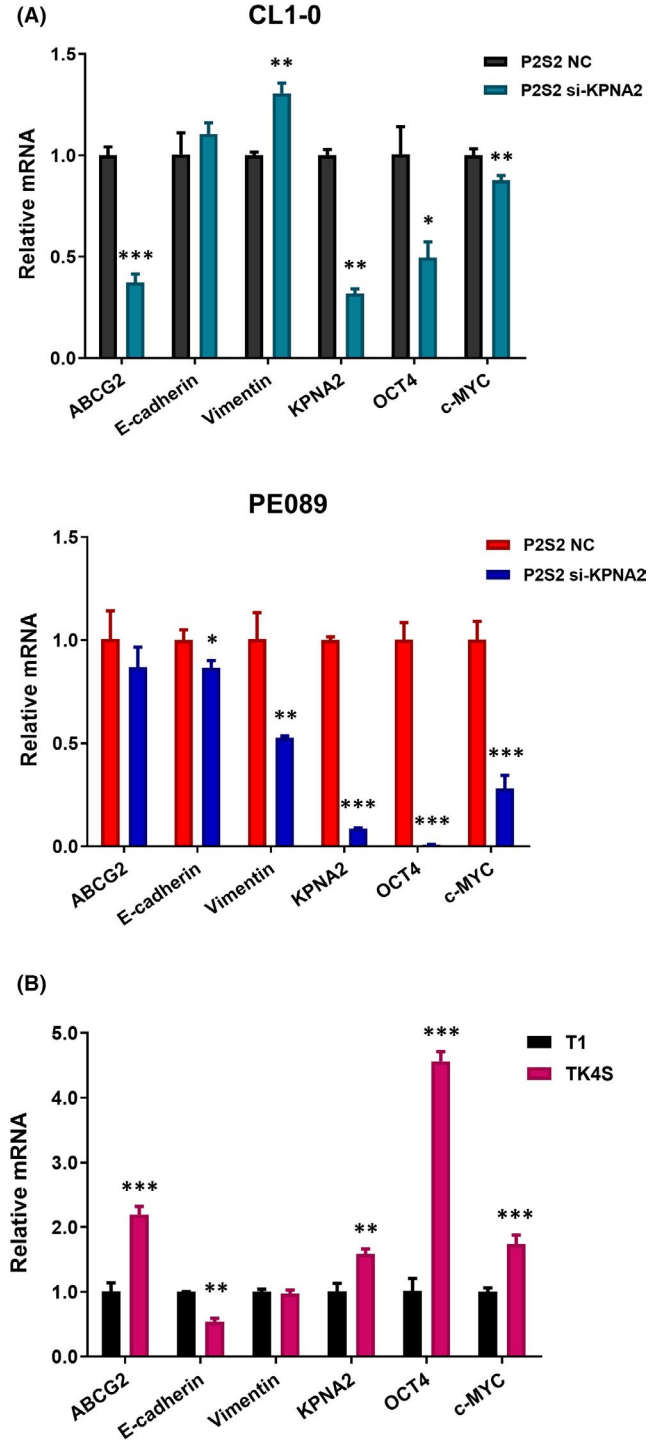

FIGURE 4 Karyopherin α2 (KPNA2) knockdown and KPNA2 expression regulate radioresistance-related gene expression. The mRNA levels of epithelial-mesenchymal transition (EMT)- and CSC-related genes in radioresistant KPNA2-knockdown P2S2 cells (A) and KPNA2-expressing CL1-0 cells (B) were measured by quantitative RT-PCR. NC, negative control siRNA. T1, tdTomato control vector. TK4S, tdTomato vector with stable expression of KPNA2. All experiments were performed in triplicate, and data are presented as the mean ± SD. $^{*}P < .05$, $^{**}P < .01$, and $^{***}P < .001$

nuclear distributions of PLSCR1 and p-STAT3 were enhanced in CL1-0 P2S2 cells compared to CL1-0 P0 cells (Figure 6A, left panel). Correlation analysis of N/C ratios, representing the subcellular localization, showed a positive correlation between KPNA2 and PLSCR1 in P2S2 cells. A positive correlation was also observed between KPNA2 and p-STAT3 (Figure 6A, right panel). The co–distribution of KPNA2 and PLSCR1-p-STAT3 in cytosolic and nuclear fractions was confirmed by subcellular fractionation assays (Figure 6B). The IP assay also revealed a positive interaction between endogenous PLSCR1 and KPNA2 in ADC cells (Figure 6C). As expected, the mRNA and protein levels of PLSCR1 and STAT1 were significantly increased in CL1-0 P2S2 cells compared with P0 cells, and the up-regulation of STAT1 and PLSCR1 in KPNA2-expressing cells was also observed (Figure 6D), suggesting that PLSCR1-STAT1 is involved in dysregulated KPNA2-mediated radioresistance. To test this possibility, we first knocked down PLSCR1 in cells with stable expression of KPNA2, and then performed a colony formation test. Figure 6E shows that PLSCR1 knockdown suppressed the radioresistance induced by the stable expression of KPNA2 in TK4S cells; this was not observed in the control T1 cells. Similar results were observed for the knockdown of PLSCR1 in cells transiently expressing KPNA2-Myc (Figure 6F). Next, to check whether these phenomena can be observed in clinical specimens, we analyzed gene expression profiles in lung ADC tissues by using the TCGA database. Among 524 lung ADC patients, 61 received radiotherapy, and 411 were documented without radiotherapy. Positive correlations were observed for PLSCR1 *vs* STAT1, KPNA2 *vs* STAT1, and KPNA2 *vs* PLSCR1 in cancerous tissues of these two patient groups (Figure 6G). Notably, the positive correlation between KPNA2 and PLSCR1 in tissues with radiotherapy ($R = 0.51$) was stronger than that detected in tissues without radiotherapy ($R = 0.26$). These results collectively suggest a positive role of the PLSCR1-STAT1 loop in KPNA2-mediated radioresistance.

3.7 | KPNA2 promotes radioresistance through a potential positive feedback loop between PLSCR1 and STAT1

To confirm the positive feedback loop between PLSCR1 and STAT1, gene knockdown of PLSCR1 or STAT1 was performed. Figure 7 shows that PLSCR1 knockdown, indeed, reduced the mRNA level of STAT1 and that STAT1 knockdown caused a reduction in PLSCR1 gene transcription in P2S2 cells. We also observed that the mRNA levels of KPNA2 were decreased in PLSCR1-knockdown and STAT1-knockdown radioresistant CL1-0 cells. The protein levels of these test genes detected by western blotting were consistent with those obtained from qRT-PCR analysis (Figure 7A and B). Given that PLSCR1 interacting with KPNA2 and PLSCR1 knockdown reversed the radiosensitivity in KPNA2-expressing cells (Figure 6), we then

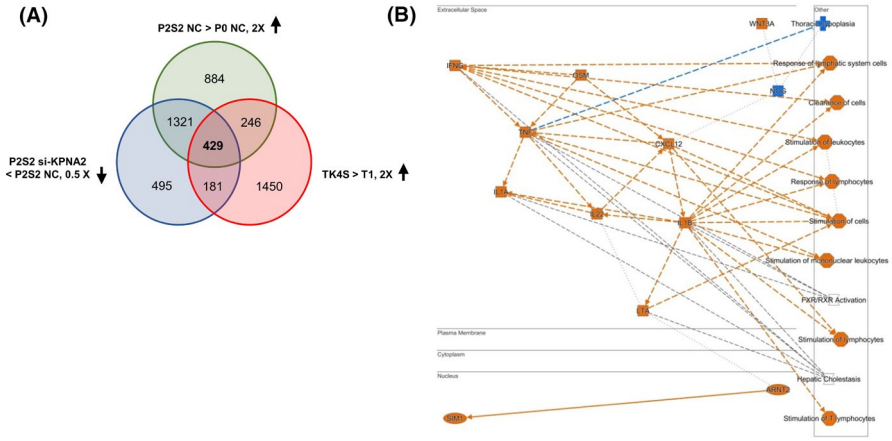

FIGURE 5 Identification of genes involved in karyopherin α2 (KPNA2)-mediated radioresistance via next-generation sequencing. (A) The intersection of differentially expressed genes (DEG) obtained by next-generation sequencing (NGS) identified 429 genes involved in KPNA2-mediated radioresistance. (B) The canonical pathways of IPA were used to identify the key pathways and functions regulated by the 429 DEGs. The blue cruciform represents diseases, and the blue square represents a growth factor. The orange octagon, square, and oval represent a function, cytokine, and transcriptional regulator, respectively. The crystal hourglass represents canonical pathways. The orange, blue, and gray dotted lines between nodes indicate activation, inhibition, and correlation or uncertainty, respectively

examined the expressions of EMT- and CSC-related genes in PLSCR1-knockdown P2S2 cells. Similar to KPNA2-knockdown cells, PLSCR1-knockdown cells showed reduced levels of ABCG2, vimentin, OCT4, and c-MYC compared to control siRNA-treated P2S2 cells (Figure 7C and D). We measured the gene and protein levels of CSC- and EMT-related factors in PLSCR1-expressing CL1-0 P0 cells. We found that the mRNA levels of ABCG2, E-cadherin, and c-MYC were upregulated in CL1-0 cells expressing Flag-PLSCR1 for 16 hours (Figure 7E, upper panel). Increased protein levels of ABCG2, E-cadherin, OCT4, and c-MYC were observed via western blotting analysis after transient expression of Flag-PLSCR1 for 24 or 40 hours (Figure 7E, lower panel). Notably, we also detected an increase in STAT1 at the mRNA and protein levels in these PLSCR1-expressing cells. Finally, our clonogenic cell survival analysis demonstrated that PLSCR1 or STAT1 knockdown reduced radioresistance in P2S2 cells (Figure 7F). These results collectively support the theory that dysregulated KPNA2 regulates the nuclear entry of PLSCR1 and, thus, sustains the positive loop between PLSCR1 and STAT1, which, in turn, enhances CSC properties and radioresistance in lung ADC cells (Figure 7G).

3.8 | AKT1 knockdown attenuates the nuclear accumulation of KPNA2 in radioresistant lung cancer cells

AKT activation promotes cell survival, proliferation, glycogen metabolism, anti–apoptosis, and DNA repair.[40] Given that the activation of the PI3K/AKT/mTOR pathway in response to radiotherapy is identified as a principal mechanism of radioresistance, inhibition of the PI3K/AKT/mTOR signaling pathway can induce radiosensitization in different types of cancer cells, including NSCLC, which has been proven in cancer cell lines, tumor xenografts, and a few phase I/II clinical trials.[41] Notably, knockdown of AKT1 but not AKT2 markedly decreased colony formation growth and migration in NSCLC cells.[42] Herein, we observed that not only enhanced nuclear distribution of pAKT (Figure 3) but also an increasing mRNA level of AKT1 were detected in P2S2 cells compared to that detected in P0 control cells (Figure 8A). To test the possibility that blocking ATK1 activity overcomes radioresistance by suppressing the nuclear accumulation of KPNA2, we silenced AKT1 expression by using a siRNA gene knockdown approach. The knockdown efficacy of AKT1 in P0 and P2S2 cells was determined by western blotting. IFA demonstrated that AKT1 knockdown reduced the nuclear distribution of KPNA2 in P2S2 cells (Figure 8B). The image quantification analysis and subcellular fractionation assays further showed that the levels of nuclear KPNA2 were decreased upon AKT1 knockdown in P2S2 cells (Figure 8C and D). This result supports the theory that suppressing the nuclear accumulation of KPNA2 may be one of the reasons for radiosensitization by inhibiting AKT1.

4 | DISCUSSION

KPNA2 has been linked with cancer invasiveness and a poor prognosis in patients, establishing KPNA2 as a potentially relevant therapeutic target.[11,12] The current study reveals a novel potential role for dysregulated KPNA2 in promoting radioresistance through modulation of CSC-associated gene expression and subcellular localization. In addition to conventional mechanisms involving ROS and DNA damage repair, several signaling pathways that regulate stress and hypoxic and immune responses in the tumor microenvironment also contribute to radioresistance.[8,43-46] In response to radiation, NBS1 is phosphorylated by ATM, and KPNA2 mediates the nuclear entry of the MRE11-RAD50-NBS1 complex for DNA repair.[47] In addition, our previous finding showed that hypoxia-induced ATM signaling promotes KPNA2 transcription in lung ADC cells.[24] We herein also

observed that the level of the DNA damage indicator γ-H2AX was dramatically increased at 2 hours after cells received 6 Gy treatment, the sublethal dose of radiation for lung ADC cells. Notably, an increasing KPNA2 expression level was observed at 24 hours after 6 Gy radiation exposure, where γ-H2AX was restored to the basal level (Figure S2). Nevertheless, KPNA2 overexpression in cancerous

TABLE 1 Potential upstream regulators involved in KPNA2-mediated radioresistance

Upstream regulator	Molecule type	*P*-value	Target molecules in dataset
TNF	Cytokine	1.09E−06	ABCB11, AGER, ANKRD55, BGLAP, C4A/C4B, CARD16, CCL20, CCN4, CD38, CD5, CD69, CLEC5A, CSGALNACT1, CXCL11, CYBA, CYP27A1, DPP4, EGFR, FERMT1, FGG, GBP4, HAS2, HNF4A, IDO1, IGFBP2, IGFL1, IL17RB, IL1R2, IL7, IRS4, KLB, KLRB1, LGALS8, LGR5, LY6D, LY96, MBL2, MET, MMP8, MUC2, MUC4, MYH7, NGF, NLRP3, NOD2, NOTCH4, NOX4, NR1I3, P2RY6, PAPPA, PCSK9, SHH, SLPI, SSTR1, SULT2A1, TAP1, TMEM40, TNFRSF11B, TNFSF11, TNR, TSLP, WFDC12, WFDC5, WNT10A, XDH
NF-κB	Complex	5.19E−04	AGER, ANXA13, CCL20, CD69, CD7, CXCL11, EGFR, FGG, HAS2, HNF4A, IDO1, IGFBP2, IGLL1/IGLL5, LTA, MBL2, MUC2, NGF, SHH, SLPI, ST18, TAP1, TNFRSF11B, TNFSF11, TSLP, WNT10A
IFNG	Cytokine	2.25E−03	AGER, AIF1, C4A/C4B, CCL20, CD1D, CD38, CLEC5A, CXCL11, CYBA, CYP27A1, DPP4, FGG, GBP4, GLDN, GRM8, HAS2, HLA-DQA1, HLA-DRB1, IDO1, IL17RB, IL18RAP, IL7, LIX1, LTA, LY96, MT1H, MUC2, MUC4, NGF, NLRP3, NOD2, NOX4, P2RY6, PAPPA, SHH, SLAMF1, SLPI, ST18, STING1, TAP1, TMOD1, TNFRSF11B, TNFSF11
OSM	Cytokine	3.51E−02	CCL20, CDSN, IL1R2, IL7, KRT16, LY6D, MMP8, NR1I3, PDZK1IP1, PTP4A1, SLPI, TAP1, TNFRSF11B, TNFSF11, WFDC12, WFDC5, XDH
STAT1	Transcription regulator	3.72E−03	C4A/C4B, CCL20, CXCL11, DPP4, GBP4, HLA-DQA1, IDO1, LY96, MUC4, NOX4, SERPINB3, SHH, SLAMF8, TAP1, TNFSF11
IL1A	Cytokine	8.33E−04	C4A/C4B, CCL20, DPP4, IL1R2, NGF, P2RY6, PDZK1IP1, SSTR1, TNFRSF11B, TNFSF11, TSLP, WFDC12, WFDC5
IL1B	Cytokine	2.11E−05	ABCB11, ACAN, AGER, AIF1, BGLAP, CCL20, CD69, CXCL11, CYBA, DPP4, FGG, HAS2, HNF1B, HNF4A, IDO1, IL18RAP, IL1R2, IL7, KLRB1, LTA, LY96, MMP8, MUC2, MUC4, NGF, NLRP7, NR1I3, PAPPA, PTP4A1, SERPINF2, SHH, SLAMF1, ST18, STMN2, TNFRSF11B, TNFSF11, TSLP, XDH
SIM1	Transcription regulator	7.21E−03	AGER, BAG6, CYBA, EGFR, GRM8, MYH7, SHH, SLC17A1, UGT1A6, ZG16
INF-α	Group	4.79E−02	CD1D, CD38, CD69, CXCL11, EGFR, IDO1, IGLL1/IGLL5, IL18RAP, IL7, LILRB4, MYH7, SHH, STAP1, TAP1
IFNA2	Cytokine	6.39E−03	CD69, CLRN3, CXCL11, DPP4, GBP4, IDO1, LILRB2, LILRB4, MET, TAP1, UGT1A6

FIGURE 6 PLSCR1 and STAT1 are positively correlated with dysregulated karyopherin α2 (KPNA2) in radioresistant cells and adenocarcinoma (ADC) cancer tissues. (A) The nuclear distributions of PLSCR1 and p-STAT3 were enhanced in P2S2 cells compared to CL1-0-P0 cells. Control P0 and radioresistant P2S2 CL1-0 cells were prepared for immunofluorescence assay (IFA) using the indicated antibodies. Scale bars: 10 μm. Correlation analysis of the N/C ratios of KPNA2 and its associated proteins (PLSCR1 and p-STAT3) in control P0 and radioresistant P2S2 cells is shown in the right panel. (B) The co–distribution of KPNA2 and PLSCR1-p-STAT3 in the cytosolic and nuclear fractions were examined by subcellular fractionation followed by western blotting using anti–KPNA2, anti–PLSCR1, and anti–phospho-STAT3 antibodies as indicated. Cy, cytosolic fraction; Nu, nuclear fraction; Wc, whole cell lysates. (C) To examine the positive interaction between KPNA2 and PLSCR1 via IP assay, cells were prepared for IP using anti–PLSCR1 antibodies and control IgG as described in the Materials and Methods. The resulting immunoprecipitated protein complexes were analyzed by western blotting using target specific antibodies as indicated. GAPDH was used as the internal control. (D) The mRNA and protein levels of STAT1 and PLSCR1 in radioresistant P2S2 cells and KPNA2-expressing CL1-0 cells were determined by quantitative RT-PCR and western blotting analysis, respectively. Triplicate qRT-PCR analyses are presented as the mean ± SD. $^{*}P < .05$, $^{**}P < .01$, and $^{***}P < .001$. (E, F) PLSCR1 knockdown suppressed the radioresistance induced by KPNA2 expression. Clonogenic survival assays were performed with exposure to different doses of radiation (0, 2, 4, and 6 Gy) after knockdown of PLSCR1 in cells with stable expression (E, TK4S *vs* T1) or transient expression (F, KPNA2-Myc *vs* VC) of KPNA2. Western blot analysis was used to determine the protein expression level and gene knockdown efficacy of target proteins. Actin was used as the internal control. NC, negative control siRNA; VC, vector control. The quantification of the clonogenic survival assays is presented in the right panel. All the data are presented as the mean ± SEM. $^{***}P < .001$ and $^{****}P < .0001$. (G) The correlations of gene sets (PLSCR1 *vs* STAT1; KPNA2 *vs* STAT1; KPNA2 *vs* PLSCR1) in TCGA lung ADC cancerous tissues were analyzed. The Spearman correlation coefficient was used to analyze the association between two genes. RT+, with radiotherapy; RT−, without radiotherapy

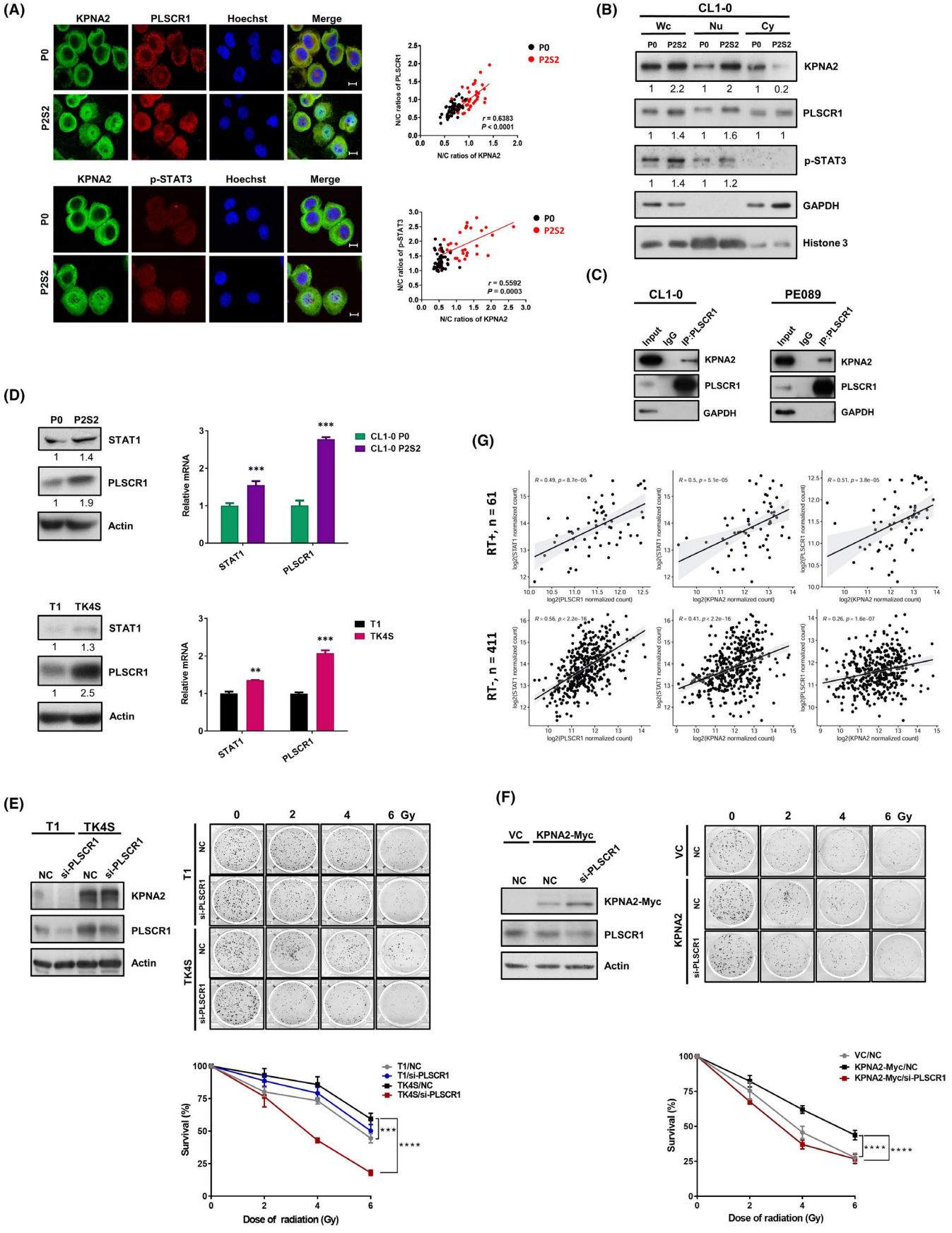
(A)
KPNA2
PLSCR1
Hoechst
Merge
P0
P2S2
N/C ratios of PLSCR1
N/C ratios of KPNA2
r = 0.6383
P < 0.0001
p-STAT3
r = 0.5592
P = 0.0003
(B)
CL1-0
Wc
Nu
Cy
KPNA2
PLSCR1
p-STAT3
GAPDH
Histone 3
(C)
CL1-0
PE089
Input
IgG
IP:PLSCR1
(D)
STAT1
Actin
Relative mRNA
CL1-0 P0
CL1-0 P2S2
T1
TK4S
(G)
RT+, n = 61
RT-, n = 411
log2(STAT1 normalized count)
log2(PLSCR1 normalized count)
log2(KPNA2 normalized count)
(E)
si-PLSCR1
KPNA2
PLSCR1
Actin
Survival (%)
Dose of radiation (Gy)
T1/NC
T1/si-PLSCR1
TK4S/NC
TK4S/si-PLSCR1
(F)
VC
KPNA2-Myc
VC/NC
KPNA2-Myc/NC
KPNA2-Myc/si-PLSCR1

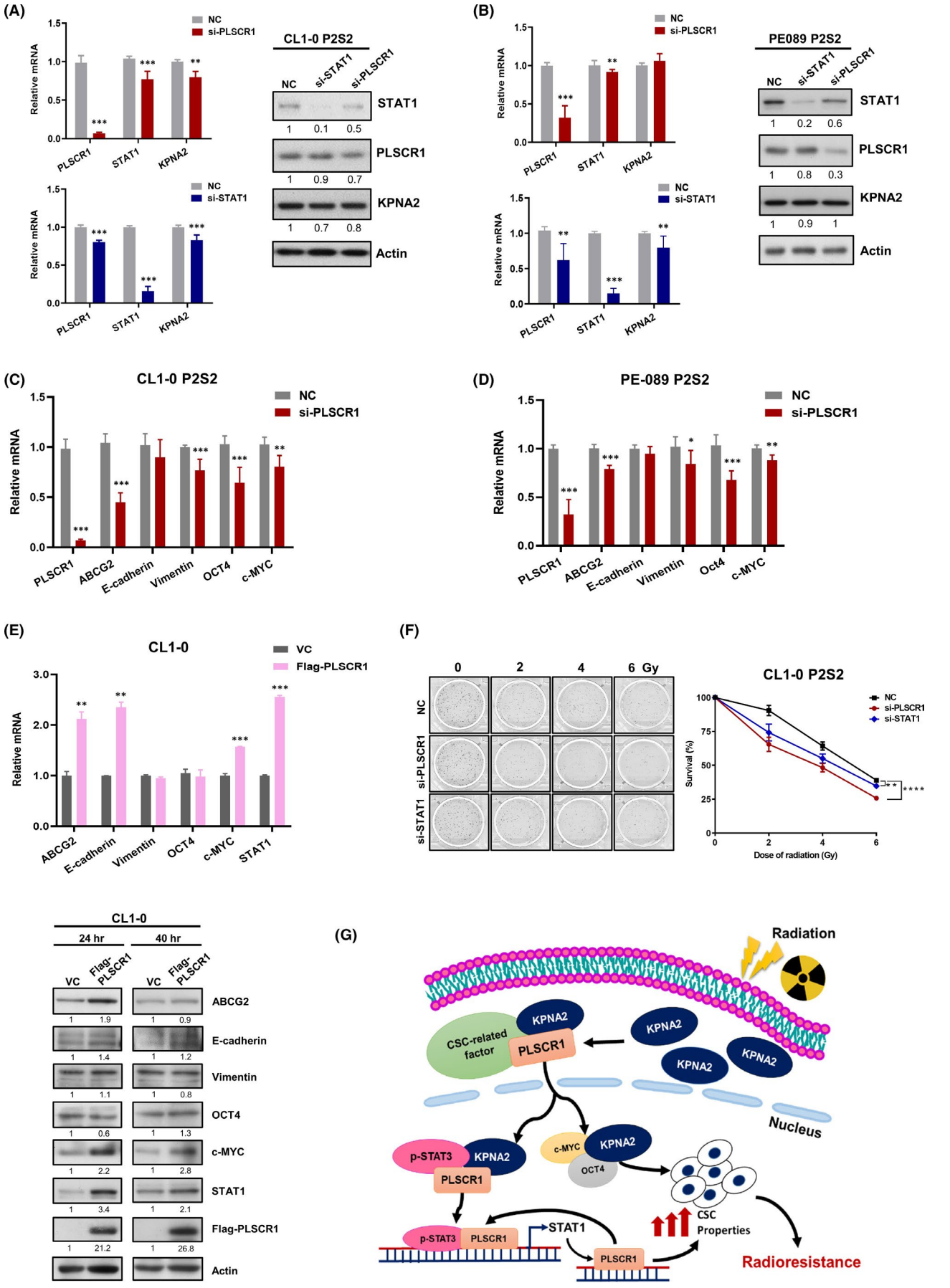
(A)
NC
si-PLSCR1
Relative mRNA
PLSCR1
STAT1
KPNA2
si-STAT1
CL1-0 P2S2
si-PLSCR1
STAT1
PLSCR1
KPNA2
Actin
(B)
PE089 P2S2
(C)
CL1-0 P2S2
PLSCR1
ABCG2
E-cadherin
Vimentin
OCT4
c-MYC
(D)
PE-089 P2S2
Oct4
(E)
CL1-0
VC
Flag-PLSCR1
STAT1
(F)
0
2
4
6 Gy
si-STAT1
CL1-0 P2S2
Survival (%)
Dose of radiation (Gy)
24 hr
40 hr
Flag-PLSCR1
(G)
Radiation
CSC-related factor
Nucleus
p-STAT3
CSC Properties
Radioresistance

FIGURE 7 Karyopherin α2 (KPNA2) may promote radioresistance through a potential positive feedback loop between PLSCR1 and STAT1. (A, B) PLSCR1 knockdown reduced the mRNA and protein levels of STAT1 and KPNA2. STAT1 knockdown reduced the mRNA and protein levels of PLSCR1 and KPNA2. CL10-P2S2 (A) and PE089 P2S2 (B) cells were transfected with siRNA as indicated. After 24 h, mRNA and protein levels of target genes were determined via quantitative RT-PCR and western blotting, respectively. (C, D) The mRNA levels of ABCG2, vimentin, OCT4, and c-MYC were reduced in PLSCR1-knockdown cells. qRT-PCR analyses are presented as the mean ± SD. $^{*}P < .05$, $^{**}P < .01$, and $^{***}P < .001$. (E) Overexpression of PLSCR1 regulated epithelial-mesenchymal transition (EMT)- and cancer stem cell (CSC)-related genes in adenocarcinoma (ADC) cells. CL1-0 cells were transfected with Flag-PLSCR1 and vector control (VC) for the indicated time. The mRNA and protein levels of EMT- and CSC-related genes were determined via qRT-PCR and western blotting, respectively. Actin was used as internal control. (F) PLSCR1 or STAT1 knockdown reduced the radioresistance in CL1-0 P2S2 cells. Clonogenic survival assays were performed on PLSCR1- or STAT1-knockdown cells after exposure to different doses of radiation (0, 2, 4 and 6 Gy). NC, negative control siRNA. The quantification of the clonogenic survival assays is presented in the right panel. All the data are presented as the mean ± SEM. $^{**}P < .01$ and $^{****}P < .0001$. (G) Proposed mechanisms by which KPNA2 promotes radioresistance in lung ADC cells. Following irradiation, KPNA2, together with its oncogenic cargo proteins, translocates into the nucleus and activates the transcription of downstream effectors, such as EMT- and CSC-related genes, which, in turn, promote radioresistance. A positive feedback loop between PLSCR1 and STAT1 may also play a crucial role in sustaining KPNA2-mediated radioresistance in lung ADC cells

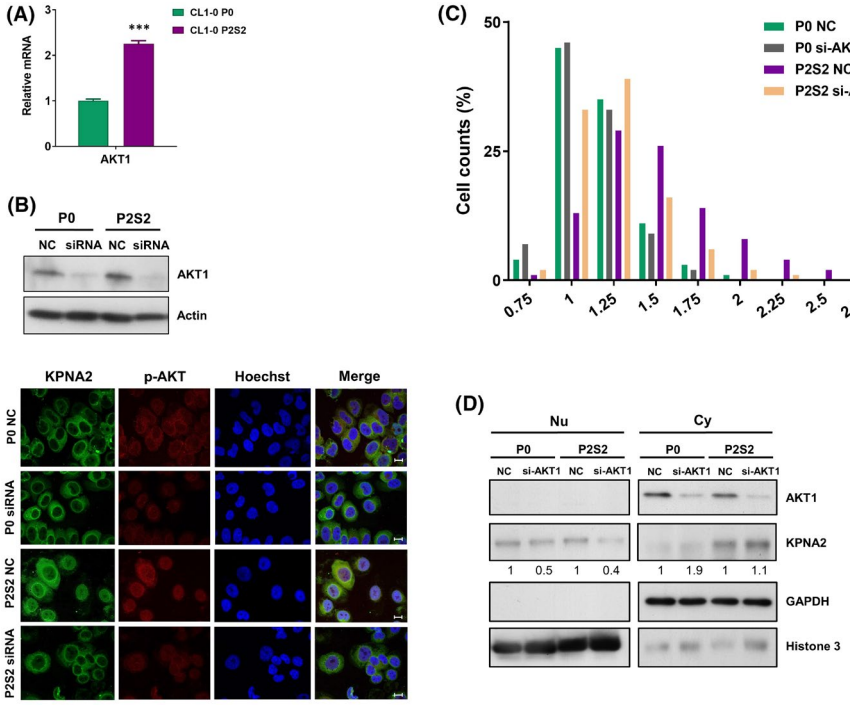

FIGURE 8 AKT1 knockdown attenuates the nuclear accumulation of karyopherin α2 (KPNA2) in radioresistant lung cancer cells. (A) The mRNA level of AKT1 was increased in P2S2 cells compared to that detected in P0 control cells. (B) AKT1 knockdown reduced the nuclear distribution of KPNA2 in radioresistant P2S2 cells. CL1-0 cells were transfected with negative control (NC) and AKT1 siRNA. After transfection for 24 h, cells were subjected to immunofluorescence assay (IFA) analysis by using antibodies as indicated. Scale bars: 10 μm. The knockdown efficacy of AKT1 in CL1-0 cells was determined through western blotting analysis. Actin was used as the internal control. (C) The distributions of KPNA2 protein in the nuclear (N) and cytoplasmic (C) fractions were analyzed under a Lionheart FX Automated Microscope. Cells were also prepared for subcellular fractionation followed by western blotting. GAPDH and histone 3 were used as loading controls for the cytosolic and nuclear fractions, respectively

tissues and its positive correlation with a poor prognosis is well documented, and we also propose that cells with inherently high KPNA2 expression along with CSC properties can be selected by radiation. This assumption is supported by our observations that both the expression level and subcellular localization of KPNA2 were dysregulated in P2S2 cells that were established by repeated 6 Gy radiation treatments at 2-week intervals, and then cells with CSC characteristics for long-term culture were selected via flow cytometric analysis. These phenomena together support the potential dual role of radiation in the induction and selection of KPNA2 expression during the development of radiation resistance.

To the best of our knowledge, we are the first to observe that radiation exposure induced KPNA2 expression in a dose-dependent manner in lung cancer cells (Figure S1A), and KPNA2 overexpression, indeed, promoted radioresistance with increasing expression of CSC-associated genes (ABCG2, OCT4, and c-MYC) accompanied by decreasing expression of the EMT-related factor E-cadherin (Figure 4B). Nuclear accumulation of KPNA2 has been observed

across cancer tissues of diverse origins.[11] It has also been documented that cellular stress, such as ultraviolet irradiation, heat shock, and oxidative stress, induces the nuclear import of KPNA2 in cervical cancer cells.[48,49] However, whether this stress-induced nuclear translocation of KPNA2 contributes to the oncogenic roles of KPNA2 remains unclear. A positive correlation between KPNA2 and OCT4 expression has been identified in NSCLC cells.[50] One recent study also showed that KPNA2 knockdown increased apoptotic cell death through inhibition of BRCA1 nuclear import following radiation exposure in breast cancer cells.[20] By virtue of KPNA2 functioning in nucleocytoplasmic transport, a possible mechanism by which KPNA2 affects radioresistance through dysregulation of the transportation of CSC-associated cargo proteins, such as OCT4, c-MYC and PLSCR1, was presented in this study. Specifically, using radioresistant cell lines as a model, the current study reveals a novel mechanism by which KPNA2 is involved in the aberrant transportation of PLSCR1 and, thus, affects the transcription of STAT1, one of the master TF in promoting radioresistance in lung ADC cells.

The microenvironment offers a favorable place for tumor cell growth and differentiation and further promotes tolerance to radiotherapy and chemotherapy.[36] Cytokines have also been revealed to be involved in CSC regulation in the cancer microenvironment.[36] In our IPA, we found that several upstream regulators were involved in KPNA2-triggered radioresistance, and most of these regulators were identified as cytokines. TNF-α has been indicated to be involved in tumor-associated macrophage and CSC signaling pathway regulation.[36] In addition, NF-κB has been shown to promote colorectal and breast CSC self-renewal, proliferation, and metastasis.[51,52] NF-κB is a KPNA2 cargo, and our previous study demonstrated that the nuclear import of NF-κB was inhibited after KPNA2 knockdown in oral cancer.[53] Further study is needed to investigate the regulation of cytokines by KPNA2 in the promotion of radioresistance in lung ADC cells.

PLSCR1, a member of the phospholipid scramblase family, is associated with multiple cellular processes, including cell proliferation, tumor suppression, transcriptional regulation, autophagy, and apoptosis.[54-58] The expression and activity of PLSCR1 are regulated by epidermal growth factor (EGF) and cytokines,[59,60] and EGF stimulation can induce the phosphorylation of PLSCR1 and its association with both EGFR and the adapter protein Shc.[61] Nuclear PLSCR1 has been shown to regulate STAT3 binding to the STAT1 promoter upon EGF treatment in breast cancer cells.[39] There are no previous studies on the expression levels or biological functions of PLSCR1 in lung cancer cells. The current study demonstrated positive correlations for PLSCR1 *vs* STAT1, KPNA2 *vs* PLSCR1, and KPNA2 *vs* STAT1 in lung ADC tissues. Endogenous PLSCR1 interacting with KPNA2 and PLSCR1 knockdown, indeed, suppressed the radioresistance induced by KPNA2 overexpression in lung ADC cells. Nevertheless, the expression levels of selected EMT- and CSC-related genes, including vimentin, E-cadherin, and OCT4 in PLSCR1-knockdown P2S2 cells and/or PLSCR1-expressing P0 cells, were not obviously different, suggesting that the unidentified factors coordinated with KPNA2-PLSCR1-STAT1 in radioresistance development. Interestingly, KPNA2 was downregulated in PLSCR1-knockdown radioresistant CL1-0 (EGFR wild-type) but not PE089 (EGFR mutation) cells (Figure 7). Some evidence has indicated that the survival of patients harboring EGFR mutations may be prolonged by oral treatment with EGFR-TKIs prior to radiotherapy.[62,63] Inhibition of the PI3K/AKT/mTOR signaling pathway induces radiosensitization in NSCLC.[41] Consistently, we found that AKT1 knockdown reduced the nuclear distribution of KPNA2 in radioresistant lung ADC cells, supporting the theory that suppressing the nuclear accumulation of KPNA2 by inhibiting AKT may be one of the mechanisms responsible for overcoming radioresistance. Given that EGF stimulation contributes to the transcriptional regulation of KPNA2 in lung ADC cells with wild-type EGFR,[64] the potential EGF-PLSCR1-KPNA2 and KPNA2-PLSCR1-STAT1 axes should be points of focus in the near future, and the accomplishment of these studies will provide mechanistic insights into radioresistance in lung ADC.

ACKNOWLEDGMENTS

We acknowledge the Bioinformatics Core Laboratory, Molecular Medicine Research Center, Chang Gung University, Taiwan for the bioinformatics analysis. We also thank Drs Chung-Pu Wu, Ko-Jiunn Liu, and Gee-Chen Chang for generously providing us with the analytic reagents and cell lines for this study.

CONFLICT OF INTEREST

The authors declare no conflicts of interest.

ORCID

Wei-Chao Liao https://orcid.org/0000-0002-4737-2675
Yu-Chin Liu https://orcid.org/0000-0002-2082-9647
Yi-Feng Chang https://orcid.org/0000-0001-5840-2051
Chun-I Wang https://orcid.org/0000-0001-8332-0162
Kwang-Huei Lin https://orcid.org/0000-0002-5649-2222
Chia-Jung Yu https://orcid.org/0000-0001-6301-7190

REFERENCES

1. Greenlee RT, Hill-Harmon MB, Murray T, Thun M. Cancer statistics, 2001. *CA Cancer J Clin*. 2001;51:15-36.
2. Shieh JM, Chiang TA, Chang WT, et al. Plumbagin inhibits TPA-induced MMP-2 and u-PA expressions by reducing binding activities of NF-kappaB and AP-1 via ERK signaling pathway in A549 human lung cancer cells. *Mol Cell Biochem*. 2010;335:181-193.
3. Erridge SC, Moller H, Price A, Brewster D. International comparisons of survival from lung cancer: pitfalls and warnings. *Nat Clin Pract Oncol*. 2007;4:570-577.
4. Maemondo M, Inoue A, Kobayashi K, et al. Gefitinib or chemotherapy for non–small-cell lung cancer with mutated EGFR. *N Engl J Med*. 2010;362:2380-2388.
5. Harrington KJ, Billingham LJ, Brunner TB, et al. Guidelines for preclinical and early phase clinical assessment of novel radiosensitisers. *Br J Cancer*. 2011;105:628-639.
6. Xia B, Zhang S, Ma S. Management of non–small cell lung cancer with EGFR mutation: the role of radiotherapy in the era of tyrosine kinase inhibitor therapy-opportunities and challenges. *J Thorac Dis*. 2017;9:3385-3393.

7. Li F, Zhou K, Gao L, et al. Radiation induces the generation of cancer stem cells: A novel mechanism for cancer radioresistance. *Oncol Lett*. 2016;12:3059-3065.
8. Lee SY, Jeong EK, Ju MK, et al. Induction of metastasis, cancer stem cell phenotype, and oncogenic metabolism in cancer cells by ionizing radiation. *Mol Cancer*. 2017;16:10.
9. Zan Y, Wang B, Liang L, et al. MicroRNA-139 inhibits hepatocellular carcinoma cell growth through down-regulating karyopherin alpha 2. *J Exp Clin Cancer Res*. 2019;38:182.
10. Goldfarb DS, Corbett AH, Mason DA, Harreman MT, Adam SA. Importin alpha: a multipurpose nuclear-transport receptor. *Trends Cell Biol*. 2004;14:505-514.
11. Christiansen A, Dyrskjøt L. The functional role of the novel biomarker karyopherin α 2 (KPNA2) in cancer. *Cancer Lett*. 2013;331:18-23.
12. Han Y, Wang X. The emerging roles of KPNA2 in cancer. *Life Sci*. 2020;241:117140.
13. Zhou LN, Tan Y, Li P, et al. Prognostic value of increased KPNA2 expression in some solid tumors: A systematic review and meta-analysis. *Oncotarget*. 2017;8:303-314.
14. Wang CI, Wang CL, Wang CW, et al. Importin subunit alpha-2 is identified as a potential biomarker for non–small cell lung cancer by integration of the cancer cell secretome and tissue transcriptome. *Int J Cancer*. 2011;128:2364-2372.
15. Wang CI, Chien KY, Wang CL, et al. Quantitative proteomics reveals regulation of karyopherin subunit alpha-2 (KPNA2) and its potential novel cargo proteins in nonsmall cell lung cancer. *Mol Cell Proteomics*. 2012;11:1105-1122.
16. Wang CI, Wang CL, Wu YC, et al. Quantitative proteomics reveals a novel role of karyopherin alpha 2 in cell migration through the regulation of vimentin-pErk protein complex levels in lung cancer. *J Proteome Res*. 2015;14:1739-1751.
17. Zeng H, Ji J, Song X, et al. Stemness related genes revealed by network analysis associated with tumor immune microenvironment and the clinical outcome in lung adenocarcinoma. *Front Genet*. 2020;11:549213.
18. Skvortsova I, Skvortsov S, Raju U, et al. Epithelial-to-mesenchymal transition and c-myc expression are the determinants of cetuximab-induced enhancement of squamous cell carcinoma radioresponse. *Radiother Oncol*. 2010;96:108-115.
19. Song KH, Jung SY, Kang SM, et al. Induction of immunogenic cell death by radiation-upregulated karyopherin alpha 2 in vitro. *Eur J Cell Biol*. 2016;95:219-227.
20. Song KH, Jung SY, Park JI, et al. Inhibition of Karyopherin-α2 Augments Radiation-Induced Cell Death by Perturbing BRCA1-Mediated DNA Repair. *Int J Mol Sci*. 2019;20:2843.
21. Chu YW, Yang PC, Yang SC, et al. Selection of invasive and metastatic subpopulations from a human lung adenocarcinoma cell line. *Am J Respir Cell Mol Biol*. 1997;17:353-360.
22. Hsu LH, Liu KJ, Tsai MF, et al. Estrogen adversely affects the prognosis of patients with lung adenocarcinoma. *Cancer Sci*. 2015;106:51-59.
23. Zhang P, Wei Y, Wang L, et al. ATM-mediated stabilization of ZEB1 promotes DNA damage response and radioresistance through CHK1. *Nat Cell Biol*. 2014;16:864-875.
24. Huang JX, Wu YC, Cheng YY, Wang CL, Yu CJ. IRF1 negatively regulates oncogenic KPNA2 expression under growth stimulation and hypoxia in lung cancer cells. *Onco Targets Ther*. 2019;12:11475-11486.
25. Li X, Sun L, Jin Y. Identification of karyopherin-alpha 2 as an Oct4 associated protein. *J Genet Genomics*. 2008;35:723-728.
26. Brognard J, Clark AS, Ni Y, Dennis PA. Akt/protein kinase B is constitutively active in non–small cell lung cancer cells and promotes cellular survival and resistance to chemotherapy and radiation. *Cancer Res*. 2001;61:3986-3997.
27. Schuurbiers OC, Kaanders JH, van der Heijden HF, Dekhuijzen RP, Oyen WJ, Bussink J. The PI3-K/AKT-pathway and radiation resistance mechanisms in non–small cell lung cancer. *J Thorac Oncol*. 2009;4:761-767.
28. Singh A, Settleman J. EMT, cancer stem cells and drug resistance: an emerging axis of evil in the war on cancer. *Oncogene*. 2010;29:4741-4751.
29. Apostolou P, Toloudi M, Chatziioannou M, Ioannou E, Papasotiriou I. Cancer stem cells stemness transcription factors expression correlates with breast cancer disease stage. *Curr Stem Cell Res Ther*. 2012;7:415-419.
30. Khodarev NN, Beckett M, Labay E, Darga T, Roizman B, Weichselbaum RR. STAT1 is overexpressed in tumors selected for radioresistance and confers protection from radiation in transduced sensitive cells. *Proc Natl Acad Sci U S A*. 2004;101:1714-1719.
31. Hui Z, Tretiakova M, Zhang Z, et al. Radiosensitization by inhibiting STAT1 in renal cell carcinoma. *Int J Radiat Oncol Biol Phys*. 2009;73:288-295.
32. Zhan JF, Chen LH, Yuan YW, et al. STAT1 promotes radioresistance of CD44(+)/CD24(-/low) cells in breast cancer. *Exp Biol Med*. 2011;236:418-422.
33. Liu S, Imani S, Deng Y, et al. Targeting IFN/STAT1 pathway as a promising strategy to overcome radioresistance. *Onco Targets Ther*. 2020;13:6037-6050.
34. Deng YR, Chen XJ, Chen W, et al. Sp1 contributes to radioresistance of cervical cancer through targeting G2/M cell cycle checkpoint CDK1. *Cancer Manag Res*. 2019;11:5835-5844.
35. Qadir AS, Ceppi P, Brockway S, et al. CD95/Fas increases stemness in cancer cells by inducing a STAT1-dependent type I interferon response. *Cell Rep*. 2017;18:2373-2386.
36. Yang L, Shi P, Zhao G, et al. Targeting cancer stem cell pathways for cancer therapy. *Signal Transduct Target Ther*. 2020;5:8.
37. Zhao KW, Li D, Zhao Q, et al. Interferon-alpha-induced expression of phospholipid scramblase 1 through STAT1 requires the sequential activation of protein kinase Cdelta and JNK. *J Biol Chem*. 2005;280:42707-42714.
38. Ben-Efraim I, Zhou Q, Wiedmer T, Gerace L, Sims PJ. Phospholipid scramblase 1 is imported into the nucleus by a receptor-mediated pathway and interacts with DNA. *Biochemistry*. 2004;43:3518-3526.
39. Huang P, Liao R, Chen X, et al. Nuclear translocation of PLSCR1 activates STAT1 signaling in basal-like breast cancer. *Theranostics*. 2020;10:4644-4658.
40. Song M, Bode AM, Dong Z, Lee MH. AKT as a therapeutic target for cancer. *Cancer Res*. 2019;79:1019-1031.
41. Wanigasooriya K, Tyler R, Barros-Silva JD, Sinha Y, Ismail T, Beggs AD. Radiosensitising cancer using Phosphatidylinositol-3-Kinase (PI3K), Protein Kinase B (AKT) or Mammalian Target of Rapamycin (mTOR) inhibitors. *Cancers*. 2020;12:1278.
42. Lee MW, Kim DS, Lee JH, et al. Roles of AKT1 and AKT2 in non–small cell lung cancer cell survival, growth, and migration. *Cancer Sci*. 2011;102:1822-1828.
43. von Essen CF. Radiation enhancement of metastasis: a review. *Clin Exp Metastasis*. 1991;9:77-104.
44. Moncharmont C, Levy A, Guy JB, et al. Radiation-enhanced cell migration/invasion process: a review. *Crit Rev Oncol Hematol*. 2014;92:133-142.
45. Wild-Bode C, Weller M, Rimner A, Dichgans J, Wick W. Sublethal irradiation promotes migration and invasiveness of glioma cells: implications for radiotherapy of human glioblastoma. *Cancer Res*. 2001;61:2744-2750.
46. Madani I, De Neve W, Mareel M. Does ionizing radiation stimulate cancer invasion and metastasis? *Bull Cancer*. 2008;95:292-300.
47. Tseng SF, Chang CY, Wu KJ, Teng SC. Importin KPNA2 is required for proper nuclear localization and multiple functions of NBS1. *J Biol Chem*. 2005;280:39594-39600.

48. Miyamoto Y, Saiwaki T, Yamashita J, et al. Cellular stresses induce the nuclear accumulation of importin alpha and cause a conventional nuclear import block. *J Cell Biol*. 2004;165:617-623.
49. Miyamoto Y, Loveland KL, Yoneda Y. Nuclear importin alpha and its physiological importance. *Commun Integr Biol*. 2012;5:220-222.
50. Li XL, Jia LL, Shi MM, et al. Downregulation of KPNA2 in non–small-cell lung cancer is associated with Oct4 expression. *J Transl Med*. 2013;11:232.
51. Liu S, Zhang C, Zhang K, et al. FOXP3 inhibits cancer stem cell self-renewal via transcriptional repression of COX2 in colorectal cancer cells. *Oncotarget*. 2017;8:44694-44704.
52. Burnett JP, Lim G, Li Y, et al. Sulforaphane enhances the anticancer activity of taxanes against triple negative breast cancer by killing cancer stem cells. *Cancer Lett*. 2017;394:52-64.
53. Wang CI, Yu CJ, Huang Y, et al. Association of overexpressed karyopherin alpha 2 with poor survival and its contribution to interleukin-1β-induced matrix metalloproteinase expression in oral cancer. *Head Neck*. 2018;40:1719-1733.
54. Shi K, An J, Qian K, et al. p53 controls the switch between autophagy and apoptosis through regulation of PLSCR1 in sodium selenite-treated leukemia cells. *Exp Cell Res*. 2020;389:111879.
55. Silverman RH, Halloum A, Zhou A, et al. Suppression of ovarian carcinoma cell growth in vivo by the interferon-inducible plasma membrane protein, phospholipid scramblase 1. *Cancer Res*. 2002;62:397-402.
56. Vinnakota JM, Gummadi SN. Two c-Myc binding sites are crucial in upregulating the expression of human phospholipid scramblase 1 gene. *Biochem Biophys Res Commun*. 2016;469:412-417.
57. Bailey K, Cook HW, McMaster CR. The phospholipid scramblase PLSCR1 increases UV induced apoptosis primarily through the augmentation of the intrinsic apoptotic pathway and independent of direct phosphorylation by protein kinase C delta. *Biochim Biophys Acta*. 2005;1733:199-209.
58. Zhou Q, Ben-Efraim I, Bigcas JL, Junqueira D, Wiedmer T, Sims PJ. Phospholipid scramblase 1 binds to the promoter region of the inositol 1,4,5-triphosphate receptor type 1 gene to enhance its expression. *J Biol Chem*. 2005;280:35062-35068.
59. Sahu SK, Gummadi SN, Manoj N, Aradhyam GK. Phospholipid scramblases: an overview. *Arch Biochem Biophys*. 2007;462:103-114.
60. Williamson P. Phospholipid scramblases. *Lipid Insights*. 2015;8:41-44.
61. Sun J, Nanjundan M, Pike LJ, Wiedmer T, Sims PJ. Plasma membrane phospholipid scramblase 1 is enriched in lipid rafts and interacts with the epidermal growth factor receptor. *Biochemistry*. 2002;41:6338-6345.
62. Lee Y, Han JY, Moon SH, et al. Incorporating erlotinib or irinotecan plus cisplatin into chemoradiotherapy for Stage III non–small cell lung cancer according to EGFR mutation status. *Cancer Res Treat*. 2017;49:981-989.
63. Park SE, Noh JM, Kim YJ, et al. EGFR mutation Is associated with short progression-free survival in patients with Stage III non–squamous cell lung cancer treated with concurrent chemoradiotherapy. *Cancer Res Treat*. 2019;51:493-501.
64. Wang CI, Chen YY, Wang CL, Yu JS, Chang YS, Yu CJ. mTOR regulates proteasomal degradation and Dp1/E2F1- mediated transcription of KPNA2 in lung cancer cells. *Oncotarget*. 2016;7:25432-25442.

SUPPORTING INFORMATION

Additional supporting information may be found in the online version of the article at the publisher's website.

How to cite this article: Liao W-C, Lin T-J, Liu Y-C, et al. Nuclear accumulation of KPNA2 impacts radioresistance through positive regulation of the PLSCR1-STAT1 loop in lung adenocarcinoma. *Cancer Sci*. 2022;113:205–220. doi:10.1111/cas.15197